Early Evaluation of Potential Environmental Impacts of Carbon Nanotube Synthesis by Chemical Vapor Deposition

DESIRÉE L. PLATA,*,†,‡ A. JOHN HART,§ CHRISTOPHER M. REDDY,‡ AND PHILIP M. GSCHWEND†

Department of Civil and Environmental Engineering, Massachusetts Institute of Technology, Cambridge, Massachusetts 02139, Department of Marine Chemistry and Geochemistry, Woods Hole Oceanographic Institution, Woods Hole, Massachusetts 02543, and Department of Mechanical Engineering, University of Michigan, Ann Arbor, Michigan 48109

Received June 3, 2009. Revised manuscript received September 15, 2009. Accepted September 22, 2009.

The carbon nanotube (CNT) industry is expanding rapidly, yet little is known about the potential environmental impacts of CNT manufacture. Here, we evaluate the effluent composition of a representative multiwalled CNT synthesis by catalytic chemical vapor deposition (CVD) in order to provide data needed to design strategies for mitigating any unacceptable emissions. During thermal pretreatment of the reactant gases (ethene and H_2), we found over 45 side-products were formed, including methane, volatile organic compounds (VOCs), and polycyclic aromatic hydrocarbons (PAHs). This finding suggests several environmental concerns with the existing process, including potential discharges of the potent greenhouse gas, methane (up to 1.7%), and toxic compounds such as benzene and 1,3-butadiene (up to 36000 ppmv). Extrapolating these laboratory-scale data to future industrial CNT production, we estimate that (1) contributions of atmospheric methane will be negligible compared to other existing sources and (2) VOC and PAH emissions may become important on local scales but will be small when compared to national industrial sources. As a first step toward reducing such unwanted emissions, we used continuous in situ measures of CNT length during growth and sought to identify which thermally generated compounds correlated with CNT growth rate. The results suggested that, in future CNT production approaches, key reaction intermediates could be delivered to the catalyst without thermal treatment. This would eliminate the most energetically expensive component of CVD synthesis (heating reactant gases), while reducing the formation of unintended byproducts.

Introduction

Recent reports have highlighted the need for improved understanding of the environmental, health, and safety risks associated with nanomaterials and their fabrication (*1*−*3*). Historically, chemical manufacturing procedures have been designed to maximize material performance and minimize production costs, but little attention has been devoted to a priori environmental impact mitigation. This practice has resulted in delayed recognition of malignant environmental effects, and at an advanced stage of industrial development, after substantial investment, it is very difficult to arrest, let alone rectify, the resultant damages. As exemplified by other industrially important materials, retarded identification of undesirable environmental impacts has necessitated costly reparation and remediation efforts (e.g., perfluorooctanoic acid from Teflon manufacture) and ultimately resulted in product bans and redevelopment of synthetic technologies (*4*−*6*). Many industrial chemicals have followed this pattern of initially rapid growth of production, recognition of malignant environmental or public health effects, subsequent material or product bans, and, finally, replacement by new technologies on a "few decades" time frame (*7*). Aware of this pattern and poised in an aggressively expanding industry, nanoscientists have a unique opportunity to alter the future approach to the development of all new materials by incorporating environmental objectives early in the design of each novel chemical process.

To provide a framework for the parallel optimization of environmental and material performance parameters, we evaluated a representative synthesis for a promising nanomaterial, vertically aligned multiwall carbon nanotubes (VA-MWCNTs). While there are several approaches to manufacturing carbon nanotubes (CNTs), the preferred method for large-volume production is catalytic chemical vapor deposition (CVD). Typical CVD procedures for CNT growth require heating a carbonaceous gas to high temperature (500−1200 °C) (*8, 9*) in a reducing or inert atmosphere (e.g., H_2 and/or He) and subsequent reaction of the heated mixture at a nanoparticle surface (e.g., Fe or Co/Mo). In combustion systems (i.e., with O_2 present), thermal treatment of carbon-based gases promotes radical formation and recombination reactions that result in the production of other volatile organic compounds (VOCs), polycyclic aromatic hydrocarbons (PAHs), and amorphous carbon or soot (*10, 11*). Similar mechanisms (i.e., radical formation and recombination) may occur in oxygen-free systems, but there is limited experimental data to support this.

Nevertheless, some of the compounds formed in reducing or inert gas conditions may raise environmental and public health concerns. In particular, photoactive VOCs have long been recognized as contributors to smog and lower atmosphere ozone formation, thereby exacerbating respiratory diseases (*12*). Furthermore, select PAHs are carcinogenic, and soot influences public respiratory health (*13*) as well as the radiative heat balance of the atmosphere (*14*). Last year, the Environmental Protection Agency (EPA) strengthened air quality standards (*15*), and several industrialized cities exceed these limits (*16*) (e.g., Houston, TX, where CNT manufacturing facilities already exist). To prevent the release of such materials, CNT manufacturers may pass their effluents through scrubbers designed to capture unacceptable levels of side-products, but a better option might be to avoid unwanted side-product formation in the first place. Hence, we sought to acquire quantitative knowledge of VOC, PAH, and particulate matter generated during CNT manufacture and to discover synthetic conditions that limit their production.

To date, publicly available effluent analyses have relied on relatively insensitive techniques, such as residual gas analysis (ppmv detection limits) (*17*−*19*). For example, online analysis of an ethyne-fed CNT production revealed a handful

* Corresponding author e-mail: dplata@alum.mit.edu.
† Massachusetts Institute of Technology.
‡ Woods Hole Oceanographic Institution.
§ University of Michigan.

10.1021/es901626p CCC: $40.75
Published on Web 10/07/2009

of incompletely identified byproducts: cyclohexane, a "cyclopentane fragment", and a "hexane fragment" (*19*). An offline analysis of a different ethyne-based CNT synthesis tentatively identified methane and several unsaturated hydrocarbons (specifically, ethene, 1-buten-3-yne, pent-3-en-1-yne, two hexadiene-yne isomers, benzene, toluene, and cyclooctatetraene) (*20*). However, trace gas components (<ppmv) that are overlooked by these methods may be released in significant quantities as the industry continues to grow. For example, annual production of CNT powders already exceeds 300 tons (*21*) (ton = 10^6 g) and is expected to double approximately every two years (*22*). If CVD processes have a 3% atom efficiency (*23*), then within 10 years, a subppmv contaminant in this effluent (that is not captured before release) could be discharged to the atmosphere in large volumes, totaling approximately 3 tons.

To avoid environmental damages from byproducts and improve resource use in VA-MWCNT production, we quantified and identified carbonaceous compounds formed by the thermal treatment of a common reaction gas mixture (C_2H_4/H_2). In our CVD reactor (Supporting Information), the growth gas mixture was heated and cooled ("preheated") before it reached the catalyst-coated silicon substrate, which was heated independently on a silicon platform in a closed quartz tube. This physical separation deconvoluted thermal effects on the feedstock gas from those on the metal catalyst and enabled investigation of the two critical processes in isolation (*24, 25*). VOCs were collected downstream of the preheater and upstream of the catalyst, and the reported gas composition represents effects of the thermal treatment only. Simultaneously, we measured VA-MWCNT height in situ using a laser displacement sensor (*25*). The mixture of thermally generated carbonaceous materials was complex and included many VOCs and PAHs, some of which may diminish CNT quality (*24*) and present environmental or toxicology concerns. Here, we estimate the potential contribution of two anticipated VA-MWCNT-based products, flat-panel displays and thermal interface materials, to current national and/or local emissions of VOCs and PAHs. With these results, we can begin to co-optimize the synthetic process by (1) minimizing unwanted side-products, (2) minimizing cost by selecting potent reagent gases that require minimal thermal treatment, and (3) maximizing production growth rates.

Experimental Methods

CNT Synthesis. To assess the effect of thermal pretreatment of reaction gases on CNT growth, we utilized a custom-built CVD reactor (*25*) in which catalyst substrate and gas temperature were controlled independently (Supporting Information). Premixed gases were heated in a quartz "preheater" tube (4 mm i.d. × 300 mm long, 75 mm heated zone). The transit time of the gas through the heated zone was roughly 130 ms, and heat transfer analysis suggested that roughly 30 ms were needed to bring the gas to the target temperature. Gas was then cooled to room temperature and delivered to a quartz reactor tube (4.8 cm i.d. × 22.9 cm long). Inside the reactor tube, VA-MWCNT thin films were grown on electron-beam deposited Fe (1.2 nm) with an Al_2O_3 (10 nm) under layer on a Si (600 um) support. The catalyst substrate temperature was controlled by a localized, resistively heated silicon platform, minimizing gas phase reactions in the reactor tube. The VA-MWCNT film height was measured in real-time using a laser displacement sensor (*25*).

To eliminate effects of tube age (*26*), preheater tubes were precombusted before each experiment. Reactant gases were introduced according to the following program: He at 2000 standard cubic centimeters per minute (sccm) for 8 min, He and H_2 at 70 and 330 sccm, respectively, for 4 min (where the substrate is turned on after 2 min), and then C_2H_4 and H_2 at 70 and 330 sccm, respectively, for the duration of the VA-MWCNT growth.

VOC Collection and Analysis. Stainless-steel 300 mL gas canisters were placed downstream from the preheater and reactor tubes. Considering the flow rate of the gases, these canisters represent a 45 s integrated signal of VOCs forming during the reaction. Gas samples were collected just after growth termination and sealed with stainless-steel ball valves.

VOCs were quantified by gas chromatography with a flame ionization detector (GC-FID; HP5890 II, HayeSep-Q, 80/100 mesh, 6′ × 1/8″ x 0.085″, 15 mL min^{-1} He carrier flow, 50 °C for 10 min, 6 °C min^{-1} to 100 °C, 8 °C min^{-1} to 160 °C, 12 °C min^{-1} to 230 °C, 7 min hold) calibrated with standard gas mixtures. Gas samples were prefocused using a cryogenic [N_2(l)] trap of Porasil-C treated silica beads. Unidentified carbonaceous species were further analyzed by GC-mass spectrometry (GC-MS; HP G1530A, DB-624, 60 m × 0.25 mm I.D. × 1.4 um film, 32 cm s^{-1}, 45 °C for 10 min, 12 °C min^{-1} to 190 °C, 2 min hold, 6 °C min^{-1} to 225 °C, 1 min hold) interfaced to a mass selective detector (HP 5873). The CO_2, He, and H_2 contents were quantified using GC-TCD (thermal conductivity detector; HP 5890 II, MoleSieve, 80/100 mesh, 6′ × 1/8″ × 0.085″, N_2 carrier gas, 70 °C isothermal).

Unfortunately, the large quantity of ethene in our samples inhibited the quantification of ethyne as the two components could not be fully resolved by gas chromatography in our system. Using mass spectral reconstruction of selected ions, we were able to confirm the presence of ethyne in these samples (as an unresolved shoulder on a large ethene peak) and estimate its concentration in one sample.

PAH Collection and Analysis. PAHs were concentrated on two consecutive polyurethane foam (PUF) filters (3″ length × 1″ diameter). These were in place for the duration of CNT growth, and the reported PAH abundances represent an integrated signal throughout the growth period. The PUF filters were downstream of two quartz fiber filters (QFFs), which collected particulate matter (>0.2 um). PUFs were precleaned by triplicate accelerated solvent extractions (ASE) with a 90:10 dichloromethane: methanol mixture at 100 °C and 1000 psi for 5 min. The same routine was used to extract PAHs from the filters. The three serial extracts were combined, concentrated by rotary evaporation, spiked with injection standards (d_{10}-phenanthrene, d_{10}-pyrene, d_{12}-chrysene) and analyzed by GC-MS (HP 6890- JEOL GCmate, HP5-MS, 30 m × 0.25 mm i.d. × 0.25 um film). Sample recovery was assessed using internal standards (d_{10}-acenaphthalene, *m*-terphenyl, and d_{12}-perylene) and ranged from 75 ± 1% for low molecular weight PAHs (128 to 154 amu) to greater than 90 ± 1% for higher molecular weight PAHs (>166 amu).

Preheater Tube Deposits and Adsorbed PAHs. Each preheater tube was sectioned into evenly spaced segments. One set of segments was used to quantify the carbonaceous deposits, and the other was used to identify sorbed compounds. Sorbed PAHs were extracted by ASE and analyzed by GC-MS (as described above). Carbonaceous deposits were analyzed by closed-tube combustion and vacuum line quantification of CO_2 (*27*). These results appear in the Supporting Information.

Results and Discussion

VOCs Formed during VA-MWCNT Synthesis: Effects of Preheater Temperature. The thermal pretreatment of VA-MWCNT reactant gases (C_2H_4/H_2 = 70/330 sccm) resulted in the formation of many VOCs (Figure 1a). None of these VOCs have been reported previously in an ethene-based CVD synthesis of CNTs, but methane, ethane, benzene, and 1-buten-3-yne have been detected in the effluents of an ethyne-fed CVD reactor (*20*). Relatively small increases in the preheater temperature led to order-of-magnitude increases in the abundances of methane, benzene, propyne,

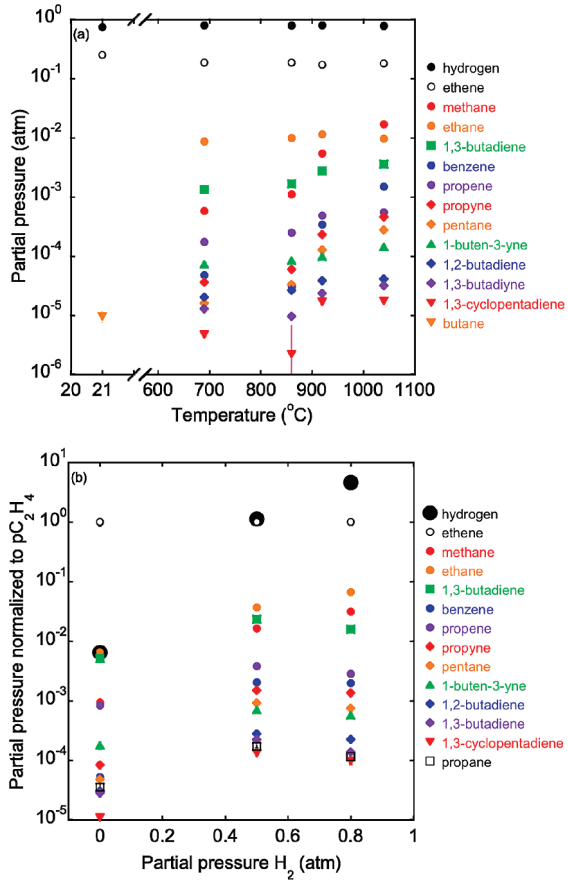

FIGURE 1. VOC abundance as a function of (a) preheater temperature (where pH_2 = 0.8 atm) and (b) partial pressure of H_2 in the feedstock gas (where the preheater temperature is 920 °C). Values represent content of the gas leaving the reactor tube, prior to any engineered attempt to filter the effluents before release to the atmosphere. Note that some H_2 was present in the post-preheater gas mixture of the pH_2 = 0 case,as some H_2 is generated from the thermal decomposition of ethene (*11*). Error bars represent one standard deviation on triplicate measurements of the same samples. Invisible error bars are smaller than the symbols.

and pentane, whereas ethane, 1,3-butadiene, and 1,2-butadiene were less sensitive to thermal treatment. VOC concentrations ranged from 4.7 ± 0.3 ppmv (1,3-cyclopentadiene) to 8700 ± 500 ppmv (ethane) at the lowest preheater temperature (690 °C) and from 17.6 ± 0.1 ppmv (1,3-cyclopentadiene) to 17000 ± 700 ppmv (methane) at the highest preheater temperature (1040 °C). Increasing preheater temperature also accelerated VA-MWCNT growth (Figure 2), so there is some motivation to use higher temperatures.

Although the effluent mixture was complex, some thermally generated compounds were correlated to the increased growth rate observed at higher preheating temperatures suggesting some VOCs may accelerate VA-MWCNT growth. In particular, there were strong correlations between the growth rate and partial pressures of methane, benzene, and 1-buten-3-yne (each with correlation coefficients of 0.99; n = 3). In our system, only the abundances of methane and ethane were sufficient to account for the mass of VA-MWCNTs formed. Although less abundant, an unsaturated compound could accelerate VA-MWCNT growth in at least two ways. Alkenes or alkynes could copolymerize with ethene at the metal catalyst, an effect that has been observed in polyethylene synthesis (*28, 29*). Alternatively, in the presence of the catalyst, methane, ethane, or ethene could react to produce a transient, unsaturated intermediate that could be incorporated rapidly into the growing CNT lattice.

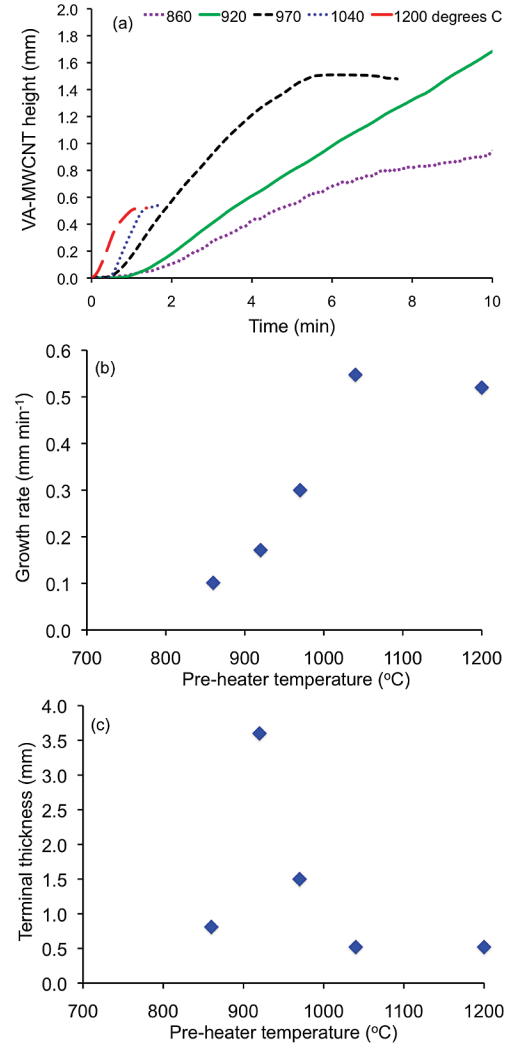

FIGURE 2. Effect of thermal pretreatment of reactant gases (H_2/C_2H_4) on VA-MWCNT growth rate and terminal height. (a) Tube growth as a function of preheater temperature (°C, shown in legend). (b) Growth rate increased with temperature until reaching a plateau above 1000 °C, while (c) terminal height of the VA-MWCNT forest exhibited a maximum at 920 °C.

Interestingly, the concentrations of the same VOCs did not correlate with the terminal CNT height, which maximized at the 920 °C preheater temperature and decreased sharply at 1040 °C (3.6 and 0.52 mm). Instead, the height was directly correlated to ethane abundance (correlation coefficient of 0.97; n = 3), suggesting that reducing conditions that lead to ethane formation also play a role in sustaining catalyst activity.

As production of such VOCs could be environmentally problematic (see below) and wasteful, these results suggest one approach for mitigating adverse environmental effluents may be to selectively deliver only the appropriate reactants to the catalyst rather than relying on thermal techniques to generate a suite of diverse reactants. Consequently, one could avoid the thermal pretreatment step and, thus, prevent the formation of potentially interfering products, minimizing unnecessary toxicant formation. This would also eliminate the most expensive component of VA-MWCNT synthesis, heating the reactant gases, which can require over 50% of the energetic demands (*30*).

VOCs Formed during VA-MWCNT Synthesis: Effects of Hydrogen Gas Content. Several reports suggest that the partial pressure of hydrogen (pH_2) in the CNT feedstock gas can influence the diameter (*31*) and purity (*32*) of CNTs.

TABLE 1. Projected Maximum Possible Emissions due to CVD Synthesis of VA-MWCNTs for Potential Applications[a]

	annual emissions (Gg yr^{-1}; Gg = 10^9 g)			
compound(s)	FPDs[b]	TIMs[b]	Houston, TX	United States
ΣVOCs	50 ± 3	0.40 ± 0.02	–[c]	16000[d]
methane[e]	1.00 ± 0.03	0.0070 ± 0.0002	–[c]	25000[f]
1,3-butadiene	2.0 ± 0.1	0.010 ± 0.001	0.68[g]	0.7[h]
benzene	0.30 ± 0.01	0.0020 ± 0.0001	1.7[g]	2.4[h]

[a] These estimates do not account for possible control technologies that could be used to filter effluents, and so they represent maximum possible releases for the studied system. Estimated emissions are compared to present day national and local emissions. The reported errors reflect propagated errors in the chemical analysis and do not reflect uncertainties associated with the projected growth of the industry. [b] Methods used to estimate emissions from VA-MWCNT synthesis for FPDs (flat-panel displays) and TIMs (thermal interface materials) are presented in the Supporting Information. Note that these estimates do not account for potential filtration technologies. [c] Data not available. [d] Environmental Protection Agency (*38*). [e] Methane is not classified as a VOC by the EPA as it is not photoactive. [f] Environmental Protection Agency (*39*). [g] All emissions sources, Environmental Protection Agency (*41*). [h] All industrial emissions sources, Environmental Protection Agency (*40*).

Hydrogen species (H•, H_2) play critical roles in gas-phase radical reactions (*11, 12, 33*), so it is reasonable to expect that changes in pH_2 will alter VOC formation. At $pH_2 = 0$, the VOC concentrations were relatively low (Figure 1b). As pH_2 increased, ethene decreased (chiefly by dilution). Ethane and methane abundance relative to ethene increased with pH_2, while all the other VOCs showed a maximum presence at mid pH_2. As observed in earlier tests of the effects of temperature, ethane concentration was correlated to VA-MWCNT terminal height (230, 1300, 1950 um for 0, 0.5, and 0.8 atm H_2, respectively; correlation coefficient of 0.98, $n = 3$). Thus, reducing conditions substantially influenced the VOCs formed as well as the terminal height of the product.

Safety Concerns and Environmental Implications of Extrapolating VOC Emissions to Industrial Scale. While preheating and varying the composition of the C_2H_4/H_2 feedstock can enable tuning of VA-MWCNT growth rate and height, several of the thermally generated VOCs can have undesirable environmental and public health effects. Of particular concern are (1) methane, a potent greenhouse gas, (2) photoactive VOCs, which contribute to smog formation, and (3) benzene and 1,3-butadiene, which are regulated as hazardous air pollutants and occupational chemical hazards by the EPA and the Occupational Safety and Health Administration (OSHA), respectively. At all of the tested preheater temperatures, benzene concentrations were over 40 times higher than time-weighted average permissible exposure limits (TWA PEL; 1 ppmv). Similarly, 1,3-butadiene concentrations exceeded the TWA PEL (1 ppmv) by over a factor of 1000, increasing from 1300 ± 100 ppmv to 3600 ± 200 ppmv over the tested preheater range. At the highest temperature, the 1,3-butadiene and benzene contents of the effluent stream are considered immediately dangerous to life and health (IDLH; limits of 2000 and 500 ppmv, respectively) (*34*). Typically, care is taken to protect employee health, and effluents are vented through fume hoods. However, if reactant mixtures with compositions like those seen in this study are discharged to the atmosphere without treatment, industrial-scale CNT synthesis may result in locally unacceptable environmental and public health consequences, and thus threaten the ultimate success of CNTs (*2*).

As the commercial market for CNT-based products is relatively nascent, there is a great deal of uncertainty surrounding the magnitude of production and details of industrial-scale synthesis. For example, CVD is favored for large-scale CNT production, but ethene may not be a preferred carbon feedstock. Additionally, some facilities make efforts to reduce emissions, while others vent all byproduct and unused reactants to the atmosphere without treatment. Acknowledging the inherent uncertainty in the future magnitude of the industry, we estimated the prospective contributions of CNT manufacture to the anthropogenic VOC flux, focusing on two potential large-scale applications of VA-MWCNTs: flat panel displays (FPDs) and thermal interface materials (TIMs). Note that the estimates presented here are values that would be released if no efforts to reduce effluent emissions were applied.

In our reactor, 0.5 cm^2 VA-MWCNTs grew to a height of 2 mm and released 0.70 ± 0.04 g VOCs ($T_{preheater}$ = 920 °C; pH_2 = 0.8 atm). We scaled this effluent mass to account for the shorter nanotubes and larger areas required by each respective VA-MWCNT application (Supporting Information). For these estimates, we assume that VA-MWCNT use will reach the same magnitude in the FPD market as liquid crystal displays (LCDs, a type of FPD) and that VA-MWCNTs will be used as TIMs in home computers (*35*). If we scale VA-MWCNT production to account for the annual LCD and home computer CPU (central processing unit) sales (in total surface area) (*36, 37*), then roughly 50 ± 3 Gg VOCs yr^{-1} and 0.40 ± 0.02 Gg VOCs yr^{-1} will be generated by FPD and TIM technologies, respectively (Table 1, note 1 Gg = 10^9 g). These emissions would represent between 0.34 and 0.002% of all the anthropogenic VOC emissions from all other sources in the United States (16 Tg yr^{-1}) (*38*), including industrial, residential, and automotive sources. The dramatic difference between the FPD and TIM estimates results from the distinct surface areas required for each, the former requiring a much larger area of VA-MWCNTs than the latter (3.8×10^{11} and 2.7×10^9 cm^2, respectively). While the total VOC output influences tropospheric ozone formation, each VOC has unique photoreactivity, toxicity, and greenhouse gas potential. Extending these estimates to individual compounds, we predict 1.00 ± 0.03 Gg yr^{-1} methane, 2.0 ± 0.1 Gg yr^{-1} 1,3-butadiene, and 0.30 ± 0.01 Gg yr^{-1} benzene would be generated from VA-MWCNT synthesis for FPDs. VA-MWCNT manufacture for TIMs would generate lesser emissions: 7.0 ± 0.2 Mg yr^{-1} methane, 10 ± 1 Mg yr^{-1} 1,3-butadiene, and 2.0 ± 0.1 Mg yr^{-1} benzene (note: 1 Mg = 10^6 g). On a national scale, these contributions are small compared to total annual emissions of methane (25000 Gg yr^{-1}) (*39*) and benzene (2.4 Gg yr^{-1}) (*40*), but could exceed emissions of 1,3-butadiene (0.7 Gg yr^{-1}) (*41*) from all other industrial sources if effluent treatment is not used. On a local scale, benzene and 1,3-butadiene releases due to VA-MWCNT manufacture for FPDs could surpass or approach the total emissions from residential and industrial releases combined. For example, in Houston, TX (one of the most industrialized cities in the United States), current total 1,3-butadiene emissions are 0.68 Gg yr^{-1}, and total benzene emissions are 1.7 Gg yr^{-1} (*41*). In contrast, contributions from VA-MWCNT-based TIMs to local VOC emissions would be marginal. Clearly, the relative impact of a CNT-based material is very sensitive to the size of the market

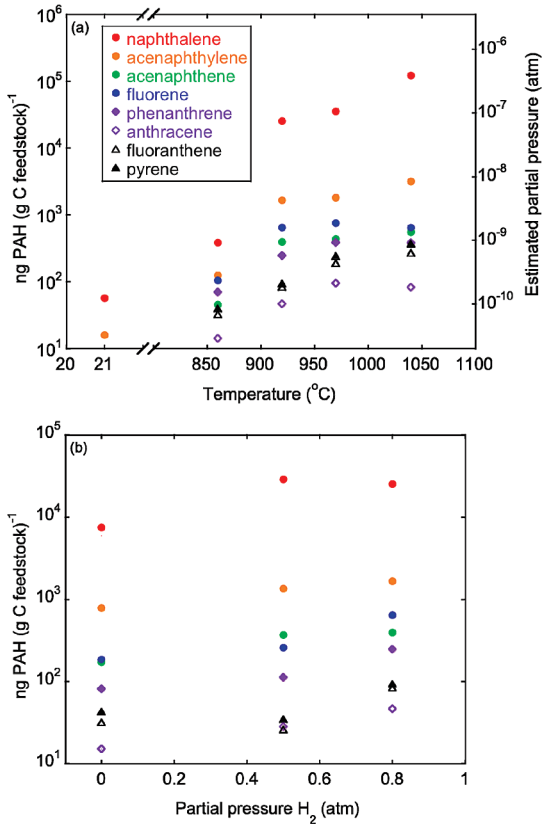

FIGURE 3. PAH content of reaction gas mixtures as related to (a) preheater temperature (where pH_2 = 0.8 atm) and (b) partial pressure of H_2 in the feedstock gas (where preheater temperature is 920 °C). Values represent the content of the gas leaving the reactor tube, prior to any engineered attempt to filter the effluents before release to the atmosphere. The sampling method concentrated PAHs over the course of the reaction, and so the PAH content is reported relative to the total amount of carbon delivered to the reactor (left-hand axis). Assuming uniform PAH production during the synthesis, we can calculate an average concentration of PAH in the effluent gas (right-hand axis in panel a), which enables comparison with NIOSH and EPA regulations. Error bars represent one standard deviation on triplicate analysis of the same sample. Invisible error bars are smaller than the symbols.

and specific application requirements (e.g., large mass or surface area), and emissions estimates should be considered for each novel technology.

PAH Formation during VA-MWCNT Synthesis: Effects of Temperature and Hydrogen Gas Content. Several PAHs, formed during VA-MWCNT synthesis, survived transit through the quartz reactor (Figure 3). Our analytical method concentrates hydrophobic PAHs over the course of the reaction, and so PAH concentrations reported here are given relative to the total amount of carbon delivered during the VA-MWCNT growth. Naphthalene was the most abundant PAH at all preheater temperatures (0.38 ± 0.4 to 12 ± 3 ug $g_{carbon\ feedstock}^{-1}$), and anthracene was the least abundant (14.2 ± 0.2 to 95 ± 20 ng $g_{carbon\ feedstock}^{-1}$).

Individual PAHs increased by orders of magnitude with increasing preheater temperature (Figure 3a). Changes in pH_2 also influenced the PAH content of the effluent, where higher PAH abundances were observed at higher pH_2 (Figure 3b). Naphthalene, fluoranthene, and pyrene production were correlated to the increasing VA-MWCNT growth rate (in temperature experiments, correlation coefficients of 0.99; n = 3). Select PAHs are thought to be important for CNT nucleation (e.g., fluoranthene) (*42*), but the role of PAHs in CNT growth (and/or inhibition) has yet to be explored experimentally. To date, online analysis of CVD reactants have had limited sensitivity (detection limits in the ppmv range), precluding the identification of trace PAH components. The preconcentration methods used in this study offer detection limits in the subparts per trillion (10^{-12}) range. Without this sensitivity, none of the PAHs formed during the tested syntheses would have been observed. Similarly, if private manufacturers use online techniques to monitor toxic formation in their reactors, they may unknowingly release PAHs to the atmosphere.

PAH Safety Concerns and Environmental Implications of Extrapolating to Industrial Scale. Many PAHs are toxic and subject to regulation by the EPA and OSHA. To determine if the PAHs formed in the reactor may present an occupational risk, we calculated the average concentration of the PAHs in the effluent stream (Figure 3a). This average was calculated from the total amount of PAH collected and total reaction time. The actual PAH concentration may have been higher or lower during a given point in the process. At the highest preheater temperature, the runtime average naphthalene content was 0.33 ± 0.01 ppmv (1.7 ± 0.1 mg m^{-3}). This does not exceed the TWA PEL (10 ppmv) (*34*), but the total PAH content of the effluent stream ($\Sigma PAH_{EPApriority}$ 1.8 ± 0.1 mg m^{-3}) was concentrated relative to engine exhaust ($\Sigma PAH_{EPApriority}$ 0.1−0.8 mg m^{-3}) (*43, 44*). Extrapolating these results and assuming no effluent treatment technologies are utilized, future PAH emissions from VA-MWCNT synthesis for FPDs and TIMs are expected to be 15 ± 0.1 and 0.11 ± 0.01 Mg yr^{-1}, respectively; emissions that are small compared to current national emissions (≥16 Gg yr^{-1}) (*45*). However, if untreated, the discharges may be important on a local scale. If so, it will be necessary to find ways to either limit PAH release to the atmosphere or minimize PAH formation. Indeed, minimizing PAH formation may prove to be beneficial, not only for the environment, but also for the quality of the CNT product (*24*).

Extension to Alternative CNT Production Methods. Within a single synthetic approach, small variations in system parameters (e.g., temperature and H/C ratio in feedstock mixture) can cause dramatic differences in the abundance and identity of the resultant byproduct. Thus, we expect that there will be substantial differences among the various methods to produce CNTs such as arc discharge, laser ablation, and CVD using alternate starting materials (e.g., CO or CH_4). Additionally, we argue that each method should be evaluated with respect to (a) energy consumption (*46*), (b) efficient starting material use (*23, 47*), and (c) the unintended byproducts formed during the synthesis. With this comprehensive comparison of environmental metrics (and simultaneous consideration of product quality), the most benign production methods can be selected at this relatively early stage.

While it would be naïve to apply inferences from a single study to other synthetic methods, it is reasonable to suggest that the high-temperature pretreatment of any gaseous hydrocarbon will lead to the production of VOCs and PAHs. Further, one might expect that higher molecular weight or more reactive starting materials (e.g., benzene or ethyne, respectively) will produce larger VOC, PAH, and soot species for a given amount of thermal energy. Similarly, less reactive compounds (e.g., methane) may produce fewer byproducts for a given amount of heat delivered. Indeed, CNTs produced by methane-based CVD often yield higher-purity CNTs, and ethyne-based syntheses often require minimal thermal treatment of the feedstock gas (e.g., by low temperature or thermal contact time) to minimize "sooting." CNT production from nonhydrocarbon feedstock gas (e.g., CO) is purported to yield very little amorphous carbon material (*48*). Arc discharge and laser ablation techniques, which rely on the

construction of CNT structures from solid graphite, might be expected to yield more solid-phase byproducts (e.g., soot).

Implications for Management of Future CNT Production. At this early stage in the growth of the CNT industry, it is possible to circumvent the potential problems from VOC and PAH release in several ways: (1) implement suitable effluent treatment technologies, (2) recycle effluents for reuse in subsequent CNT syntheses by removing trace contaminants, recollecting critical feedstock components, and generating energy onsite from appropriate materials (e.g., H_2), and/or (3) reduce the formation of compounds of concern through modified synthetic approaches. The first approach requires little-to-no technological development, and effluent treatment and recycling are already in use in several high-volume CVD production facilities in the United States and Europe. The third approach may further reduce emissions (and save energy), but it still requires iterative collaboration between materials scientists and environmental chemists. This data set enables the first steps toward such improved synthetic techniques.

Armed with a thorough description of the thermally derived products, we can begin to consider which compounds are most active as CNT precursors. For example, compounds that were correlated with CNT formation rates (e.g., 1-buten-3-yne) should be directly administered to CNT catalyst to determine if satisfactory growth can be achieved without thermal treatment of feedstock gases. Indeed, this is the subject of a separate study of VOCs as CNT-forming reactants (*49*). By selecting the appropriate gaseous component(s) as starting materials, instead of relying on thermal generation of the compounds, one may substantially improve resource use during VA-MWCNT synthesis. In particular, (1) reaction efficiency may improve, (2) chemical and energetic costs will be greatly reduced, (3) amorphous carbon formation may decrease, thereby increasing the purity and performance of the product, (4) formation of undesirable compounds of environmental concern will be reduced, and (5) future cleanup and public health reparations will be avoided.

Acknowledgments

The authors thank the WHOI Ocean Ventures Fund, Seaver Institute, Chesonis Family via the MIT Earth System Initiative, and Martin Family Society of Fellows for Sustainability. We are grateful for J.S. Seewald, E. Reeves, S.P. Sylva, R.K. Nelson, G.D. Nessim, A. Slocum, B. Wardle, and C.V. Thompson for useful discussions and resources.

Supporting Information Available

Reactor design and sampling approach, PAHs retained on room-temperature reactor walls, scaling VA-MWCNT production to potential markets, PAH ratios and unique isomer present in effluent, solid carbon formation during VA-MWCNT synthesis, additional carbonaceous materials in effluent, and analytical approach used to identify compounds formed during CVD. This material is available free of charge via the Internet at http://pubs.acs.org.

Literature Cited

(1) Hutchison, J. E. Greener Nanoscience: A proactive approach to advancing applications and reducing implications of nanotechnology. *ACS Nano* **2008**, *2* (3), 395–402.

(2) Maynard, A. D.; Aitken, R. J.; Butz, T.; Colvin, V.; Donaldson, K.; Oberdörster, G.; Philbert, M. A.; Ryan, J.; Seaton, A.; Stone, V.; Tinkle, S. S.; Tran, L.; Walker, N. J.; Warheit, D. B. Safe handling of nanotechnology. *Nature* **2006**, *444*, 267–269.

(3) Federal Research Plan Inadequate to Shed Light on Health and Environmental Risks Posed by Nanomaterials. *National Academy of Sciences News Office*, , 2008.

(4) DuPont Progress Report on PFOA Phase Out, 2008. http://www2.dupont.com/PFOA2/en_US/assets/downloads/pdf/PFOAReportExecSummary_20080114.pdf, 2008.

(5) EPA Announces Substantial Decrease of PFOA, 2008. U.S. Environmental Protection Agency. http://yosemite.epa.gov/opa/admpress.nsf/68b5f2d54f3eefd28525701500517fbf/8f9dbdd044050f71852573e50064439f!OpenDocument.

(6) New DuPoont Capstone for Repellents and Surfactants Deliver Maximum Performance, Minimal Environmental Footprint. 2008. DuPont. http://www2.dupont.com/Capstone/en_US/assets/downloads/final_press_release_english_3_20_2008.pdf.

(7) Schwarzenbach, R. P.; Gschwend, P. M.; Imboden, D. M. *Environmental Organic Chemistry*, 2nd ed.; John Wiley and Sons: New York; 2003.

(8) See, C. H.; Harris, A. T. A review of carbon nanotube synthesis via fluidized-bed chemical vapor deposition. *Ind. Eng. Chem. Res.* **2007**, *46*, 997–1012.

(9) Lamouroux, E.; Serp, P.; Kalck, P. Catalytic routes towards single wall carbon nanotubes. *Catalysis Rev.* **2007**, *49*, 341–405.

(10) Richter, H.; Howard, J. B. Formation of polycyclic aromatic hydrocarbons and their growth to soot- a review of chemical reaction pathways. *Prog. Energy Combust. Sci.* **2000**, *26*, 565–608.

(11) Towell, G. D.; Martin, J. J. Kinetic data from nonisothermal experiments: Thermal decomposition of ethane, ethylene, and acetylene. *AIChE. J.* **1961**, *7* (4), 693–698.

(12) National Research Council . Vapor-Phase Organic Pollutants: Volatile Hydrocarbons and Oxidation Products, In *Medical and Biological Effects of Environmental Pollutants*; National Academy of Sciences: Washington, DC, 1976.

(13) National Research Council. Airborne Particles, In *Medical and Biological Effects of Environmental Pollutants*; University Park Press, National Academy of Sciences: Baltimore, MD, 1979.

(14) Kaufman, Y. J.; Fraser, R. S. The effect of smoke particles on clouds and climate forcing. *Science* **1997**, *277*, 1636–1639.

(15) *National Ambient Air Quality Standards for Ozone*; 40 CRF Parts 50 and 58, Final Rule; U.S. Environmental Protection Agency: Washington, DC, 2008; http://www.epa.gov/fedrgstr/EPA-AIR/2008/March/Day-27/a5645.pdf.

(16) Counties with Monitors Violating the 1997 8-h Ozone Standard of 0.08 ppm (based on 2004−2006 Air Quality Data), 2008. U.S. Environmental Protection Agency. http://www.epa.gov/air/ozonepollution/pdfs/2003-2005_Design_Value_Color.pdf, http://www.epa.gov/air/ozonepollution/pdfs/2008_03_monitors_violating_1997.pdf, 2008.

(17) Ago, H.; Uehara, N.; Yoshihara, N.; Tsuji, M.; Yumura, M.; Tomonaga, N.; Setoguchi, T. Gas analysis of the CVD process for high yield growth of carbon nanotubes over metal-supported catalysts. *Carbon* **2006**, *44*, 2912–2918.

(18) Tian, Y.; Hu, Z.; Yang, Y.; Chen, X.; Ji, W.; Chen, Y. Thermal analysis-mass spectroscopy coupling as a powerful technique to study the growth of carbon nanotubes from benzene. *Chem. Phys. Lett.* **2004**, *388*, 259–262.

(19) Kim, S.-M.; Zhang, Y.; Teo, K. B. K.; Bell, M. S.; Gangloff, L.; Wang, X. L.; Milne, W. I.; Wu, J.; Jiao, J.; Lee, S.-B. SWCNT growth on Al/Fe/Mo investigated by in situ mass spectroscopy. *Nanotechnology* **2007**, *18*, 185709(6).

(20) Schmitt, T. C.; Biris, A. S.; Miller, D. W.; Biris, A. R.; Lupu, D.; Trigwell, S.; Rahman, Z. U. Analysis of effluent gases during the CCVD growth of multi-wall carbon nanotubes from acetylene. *Carbon* **2006**, *44*, 2032–2038.

(21) Eklund, P. C.; Ajayan, P. M.; Blackmon, R.; Hart, A. J.; Kong, J.; Pradhan, B.; Rao, A.; Rinzler, A. G. *International Assessment of Research and Development on Carbon Nanotubes: Manufacturing and Applications*; World Technology Evaluation Center Final Report; 2008; http://www.wtec.org/cnm.

(22) Thayer, A. M. Carbon nanotubes by the metric ton. *Chem. Eng. News* **2007**, *85* (46), 29–35.

(23) Healy, M. L.; Dahlben, L. J.; Isaacs, J. A. Environmental assessment of single-walled carbon nanotube processes. *J. Ind. Ecol.* **2008**, *12* (3), 376–393.

(24) Meshot, E. R.; Plata, D. L.; Tawfick, S.; Zhang, Y. Y.; Verploegen, E. A.; Hart, A. J. Engineering vertically aligned carbon nanotube growth by decoupled thermal treatment of precursor and catalyst. *ACS Nano* **2009**, *3* (9), 2477–2486.

(25) Hart, A. J.; van Laake, L. C.; Slocum, A. H. Desktop growth of carbon nanotube monoliths with in situ optical imaging. *Small* **2007**, *3* (5), 772–777.

(26) Liu, K.; Liu, P.; Jiang, K.; Fan, S. Effect of carbon deposits on the reactor wall during the growth of multi-walled carbon nanotube arrays. *Carbon* **2007**, *45*, 2379–2387.

(27) McNichol, A. P.; Osborne, E. A.; Gagnon, A. R.; Fry, B.; Jones, G. A. TIC, TOC, DIC, DOC, PIC, POC- unique aspects in the preparation of oceanographic samples for ^{14}C-AMS. *Nucl. Instrum. Methods Phys. Res.* **1994**, *B92* (1−4), 162–165.

(28) Choi, K. Y.; Ray, W. H. Polymerization of olefins through heterogeneous catalysis. II. Kinetics of gas phase propylene polymerization with Ziegler−Natta catalysts. *J. Appl. Polym. Sci.* **1985**, *30*, 1065–1081.
(29) Jaber, I. A.; Ray, W. H. Polymerization of olefins through heterogeneous catalysis. XIV. The influence of temperature in the solution copolymerization of ethylene. *J. Appl. Polym. Sci.* **1993**, *50*, 201–215.
(30) Branham, M. Semiconductors and sustainability: Energy and materials use in integrated circuit manufacturing. Master's Thesis, Massachusetts Institute of Technology, Cambridge, MA, 2008.
(31) Okita, A.; Suda, Y.; Oda, A.; Nakamura, J.; Ozeki, A.; Bhattacharyya, K.; Sugawara, H.; Sakai, Y. Effects of hydrogen on carbon nanotube formation in CH_4/H_2 plasmas. *Carbon* **2007**, *45*, 1518–1526.
(32) Jungen, A.; Stampfer, C.; Durrer, L.; Helbling, T.; Hierold, C. Amorphous carbon contamination monitoring and process optimization for single-walled carbon nanotube integration. *Nanotechnology* **2007**, *18*, 075603.
(33) Stein, S. E.; Fahr, A. High-temperature stabilities of hydrocarbons. *J. Phys. Chem.* **1985**, *89* (17), 3714–3725.
(34) *NIOSH Pocket Guide to Chemical Hazards*; Centers for Disease Control and Prevention, National Institute for Occupational Safety and Health: Washington, DC, 2005.
(35) Dean, K. A. A new era: Nanotube displays. *Nat. Photonics* **2007**, *1* (5), 273–275.
(36) *Global Market Information Database: Consumer Electronics*; Euromonitor International: London, 2007.
(37) *An Assessment on the Future of Carbon Nanotubes- Strategic Analysis of the Market and Potential*; Frost and Sullivan, Ltd.: New York, 2006.
(38) National Air Quality and Emissions Trends Report, 2003 Special Studies Edition; U.S. Environmental Protection Agency: Research Triangle Park, NC, 2003; pp 9−47; http://www.epa.gov/air/airtrends/aqtrnd03/.
(39) Methane Sources and Emissions, 2003. U.S. Environmental Protection Agency. http://www.epa.gov/methane/sources.html.
(40) Toxics Release Inventory, 2006. U.S. Environmental Protection Agency. http://www.epa.gov/tri/.
(41) Hanna, S.; Paine, R.; Heinold, D.; Kintigh, E.; Frey, H. C.; Baker, D.; Karp, R. Uncertainties in Benzene and 1,3-Butadiene Emissions in Houston and Their Effects on Uncertainties in Concentrations Calculated by AERMOD and ISC, U.S. Environmental Protection Agency. http://www.epa.gov/ttn/chief/conference/ei13/uncertainty/hanna.pdf (accessed April 2008).
(42) Eres, G.; Kinkhabwala, A. A.; Cui, H.; Geohegan, D. B.; Puretzky, A. A.; Lowndes, D. H. Molecular beam-controlled nucleation and growth of vertically aligned single-wall carbon nanotube arrays. *J. Phys. Chem. B.* **2005**, *109* (35), 16684–16694.
(43) Chen, Y.-C.; Lee, W.-J.; Uang, S.-N.; Lee, S.-H.; Tsai, P.-J. Characteristics of polycyclic aromatic hydrocarbon (PAH) emissions from a UH-1H helicopter engine and its impact on the ambient environment. *Atmos. Environ.* **2006**, *40*, 7589–7597.
(44) Mi, H.-H.; Lee, W.-J.; Chem, C.-B.; Yang, H.-H.; Wu, S.-J. Effect of fuel aromatic content on PAH emission from a heavy-duty diesel engine. *Chemosphere* **2000**, *41*, 1783–1790.
(45) Galarneau, E.; Makar, P. A.; Sassi, M.; Diamond, M. L. Estimation of atmospheric emissions of six semivolatile polycyclic aromatic hydrocarbons in southern Canada and the United States by use of an emissions processing system. *Environ. Sci. Technol.* **2007**, *41*, 4205–4213.
(46) Isaacs, J. A.; Tanwani, A.; Healy, M. L. Environmental assessment of SWNT production. *Proc. IEEE Smyp. Electron. Environ.* **2006**, 38–41,, DOI: 10.1109/ISEE.2006.1650028.
(47) Robichaud, C. O.; Tanzil, D.; Weilenmann, U.; Wiesner, M. R. Relative risk analysis of several manufactured nanomaterials: An insurance industry context. *Environ. Sci. Technol.* **2005**, *39* (22), 8985–8994.
(48) Nikolaev, P.; Bronikowski, M. J.; Bradley, R. K.; Rohmund, F.; Colbert, D. T.; Smith, K. A.; Smalley, R. E. Gas-phase catalytic growth of single-walled nanotubes from carbon monoxide carbon. *Chem. Phys. Lett.* **1999**, *313*, 91–97.
(49) Plata, D. L. Carbon Nanotube Synthesis and Detection: Limiting the Environmental Impact of Novel Technologies. Ph.D. Dissertation, Massachusetts Institute of Technology: Cambridge, MA, 2009; Chapter 5.

ES901626P

Supporting Information for: "Early evaluation of potential environmental impacts of carbon nanotube synthesis by chemical vapor deposition"

Desirée L. Plata[1,2], A. John Hart[3], Christopher M. Reddy[2], Philip M. Gschwend[1]*

[1]R.M. Parsons Laboratory, Department of Civil and Environmental Engineering, Massachusetts Institute of Technology, Cambridge, MA 02139
[2]Department of Marine Chemistry and Geochemistry, Woods Hole Oceanographic Institution, Woods Hole, MA 02543
[3]Department of Mechanical Engineering, University of Michigan, Ann Arbor, MI 48109
*corresponding author: dplata@alum.mit.edu

This document includes (13 pages):

Section S1: *Reactor design and sampling approach*

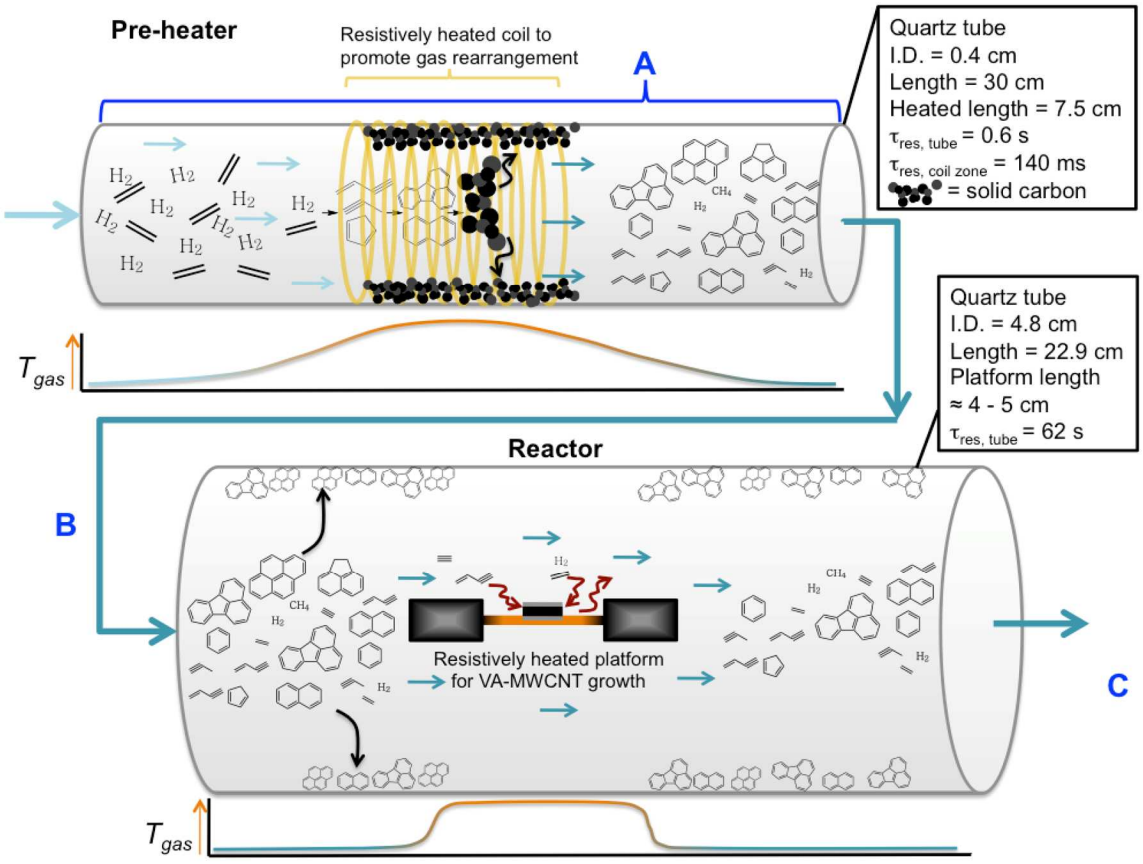

Figure S1. Reactor design and sampling of thermally generated species during transport through a two-stage CVD process, where the reactant gases were thermally treated in pre-heater. Chemical structures, particles, and quartz tubes are not drawn to scale. Hydrogen and ethylene were introduced to a narrow-diameter (4 mm) pre-heater tube that was wrapped with a resistively heated coil and covered with insulating material (insulation not shown). At high temperatures (*e.g.*, 690 – 1200°C), ethylene and hydrogen rearrange and form other molecules (*e.g.*, methane, 1,3-butadiene, benzene, and fluoranthene) and soot-like particles. Solid carbon deposits formed in the heated zone of the pre-heater tube, but were not deposited significantly outside of the heated zone. Sampling zone A was sectioned along the flow axis prior to quantification of solid carbon deposits. VOCs and PAHs survived transit through the pre-heater tube and were delivered to a room-temperature reactor. Here, PAHs were lost from the reactant stream (see Figure S2) due to sorption to the cool quartz walls of the reactor. Some PAHs were transported out of the reactor as effluent. VOCs were not retained on the reactor walls, and comparisons at sampling points B and C did not show distinct differences. VOC and PAH abundances presented in subsequent figures of the text represent samples collected at sampling points B and C, respectively. Both PAHs and VOCs were available for carbon nanotube growth on the resistively heated platform, which supported a VA-MWCNT catalyst substrate.

Section S2: *PAHs were retained on room temperature walls of the quartz reactor tube*

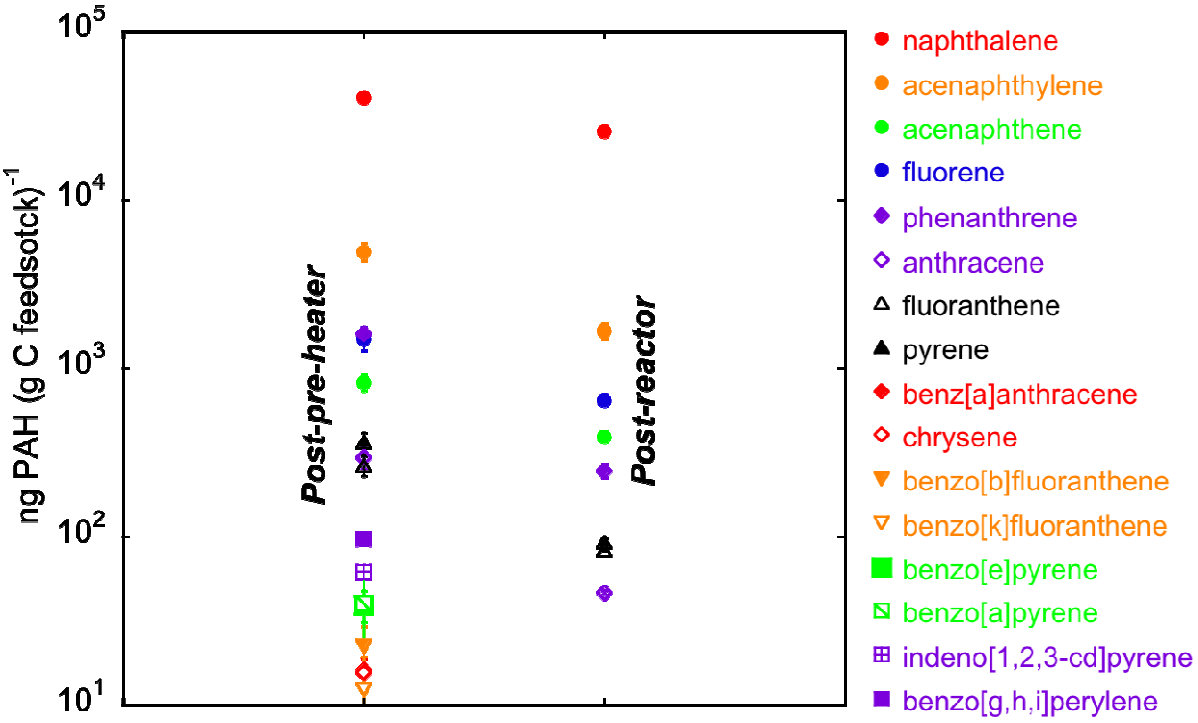

Figure S2. Polycyclic aromatic hydrocarbon content of gases exiting the pre-heater tube (post-pre-heater) and exiting the reactor (post-reactor). Several compounds, benzo[*b*]fluoranthene, benzo[*k*]fluoranthene, benzo[*e*]pyrene, benzo[*a*]pyrene, indeno[*1,2,3-cd*]pyrene, and benzo[*g,h,i*]perylene, were formed in the pre-heater, but did not survive transit through the reactor tube. The total abundance of other PAHs decreased as the gas mixture traveled through the reactor tube. The total mass loss of the PAHs was small compared to the mass of CNTs formed. Error bars are one standard deviation on triplicate measurements.

Section S3: *Scaling VA-MWCNT production to potential markets*

To make the following estimates, we assumed that VA-MWCNT use will reach the same magnitude in FPDs as liquid crystal displays (LCDs) and that VA-MWCNTs will be used as thermal interface materials (TIMs) over the central processing units (CPUs) in home computers. Note that LCDs are competitive in terms of cost and performance, and substantial advances in CNT technology are still required before VA-MWCNT FPDs become a commercial reality. VA-MWCNT TIMs are in the early stages of development, but they are very promising. If ultimately successful, their market applications will extend to all electronics, not just home computers.

In both estimates (for LCDs and TIMs), we assume that relatively short (≤100 um) VA-MWCNT forests will suffice. This would require roughly $1/10^{th}$ of the actual growth time, and we reduce our emissions by a factor of 10 to account for the truncated growth. We then calculate the average mass of ethylene that is delivered during that time, and knowing the mass of each compound per gram of ethylene (for a 920 ^{o}C growth), we determine the mass of each compound that will be formed during the production of 0.5 cm^2 of VA-MWCNTs. This area is scaled up to account for the total surface area of the two applications described here:

(1) Scaling VA-MWCNT production to the size of the current liquid crystal display market

LCD technology accounts for a fraction (90% of dollar revenues in 2005) of the current flat panel display market. Annual sales of LCDs are recorded as the number of unit sales according to diagonal display size and type (*e.g.*, television or laptop). Assuming an aspect ratio (*e.g.*, 4:3 or 16:9), we calculated the total area of each display and multiplied by a factor to account for the total number of sales. Once we know the total area of LCD flat panel displays, we assumed that VA-MWCNT-based displays will reach the magnitude of the LCD market. Then, the emissions generated to synthesize a given area of VA-MWCNTs were scaled to account for the total display area of the market.

Sample calculation: Here, we assume an aspect ratio of 16:9.

Table S1. Converting total liquid crystal display unit sales to total area.

Diagonal screen size[a] (in)	% of market[a]	Total area (cm^2)
LCD Television Screens (5.8×10^7 units)		
40	7	1.8×10^{10}
37	15	3.3×10^{10}
32	28	4.6×10^{10}
30	50	7.2×10^{10}
	Subtotal	*1.69×10^{11}*
LCD Monitor Screens (2.35×10^8 units)		
27	5	2.4×10^{10}
19	39	9.1×10^{10}
17	44	8.2×10^{10}
15	12	1.8×10^{10}
	Subtotal	*2.15×10^{11}*
Other[b] (1.1×10^7 units)		
4	100	4.9×10^8
	Subtotal	*4.9×10^8*
	Total area of LCD displays	***3.8×10^{11}***

[a]Data from Frost & Sullivan using sales in 2007 (projected from base year of 2005) .
[b]This category includes mobile phones, medical, public information, and automotive displays. An average diagonal screen size of 4" was assumed.

If we assume an aspect ratio of 4:3, the total LCD area becomes 4.3×10^{11} cm^2. The calculations presented in the manuscript text assume a 16:9 aspect ratio. Multiplying those estimates by 1.1 ($4.3 \times 10^{11} / 3.8 \times 10^{11}$) gives the emission output that would be calculated by assuming a 4:3 aspect ratio, putting bounds on the error induced by the aspect ratio assumption.

Note that these estimates are very sensitive to the VA-MWCNT area-to-effluent mass ratio. In our study, the reactor geometry was optimized to synthesize 0.5 cm^2 VA-MWCNTs, and novel reactor geometries may enable larger areas for a given effluent quantity. The largest area of CNTs synthesized in an array for a flat panel display was ~70 cm^2 (Coll *et al.*). As an exercise, we can make the grand (unjustified) assumption that the same effluent quantity was released during that synthesis. Then, the estimates presented in the manuscript text would be overestimated by a factor of 140 (70 cm^2/0.5 cm^2).

(2) Scaling VA-MWCNT production to the size of the current household computer central processing unit (CPU) market

Annual sales of household computers were 134,826,800 in 2007 (Euromonitor International). The average household computer contains between 1 and 3 cm^2 CPU, and so we assumed a moderate value of 2 cm^2 (personal communication, Intel®). Then, we assume that the VA-MWCNT density must be at least 10% of the total surface area occupied by the forest. As-grown VA-MWCNTs in our system have a forest density of approximately 1%, and this density can be increased by squeezing the forest down to $1/10^{th}$ of its original size. Thus, the necessary area of VA-MWCNTs is 10-times larger than the area of CPUs sold globally. Then, the area of CPUs in home computers is 2.7×10^8 cm^2, and the area of VA-MWCNT forests needed to act as efficient TIMs is **2.7×10^9 cm^2.**

Section S4: ***PAH ratios and unique PAH isomer present in the CVD effluent.***

There are several sources of PAHs to the environment, and diagnostic PAH ratios have been used to indicate the origin and formation temperature of PAHs (Gschwend and Hites). Fluoranthene/pyrene ratios from VA-MWCNT synthesis were between 0.7 and 0.8, very similar to those found in urban aerosols (0.6 to 0.8), and phenanthrene/anthracene ratios were between 4 and 5, consistent with pyrogenic PAH formation (phenanthene/anthracene < 10) (Lima *et al.*, Budzinski *et al.*). High-temperature processes (*i.e.*, > approximately 800^oC) often favor non-alkylated PAH formation, and methylated PAH-to-parent PAH ratios from VA-MWCNT synthesis were low, as expected, decreasing from 0.38 to 0.06 with increasing pre-heater temperature.

While VA-MWCNT-derived PAH ratios are not distinct from other high-temperature processes, there were some unique compounds in the CVD effluent stream that may be useful for tracking emissions. Acephenanthrylene, an isomer of fluoranthene and pyrene, is rarely observed in the natural world (Yunker *et al*.). The presence of this unique isomer in VA-MWCNT effluent may be useful for tracing CVD reactant streams near the point-of-release. We tentatively identified acephenanthrylene in the VA-MWCNT effluent using relative retention times and mass spectra, and we are working to confirm the compounds identity using

commercial standards. However, the atmospheric lifetime of these chemicals must be explored before they can offer conclusive information about PAH sources in aged environmental samples.

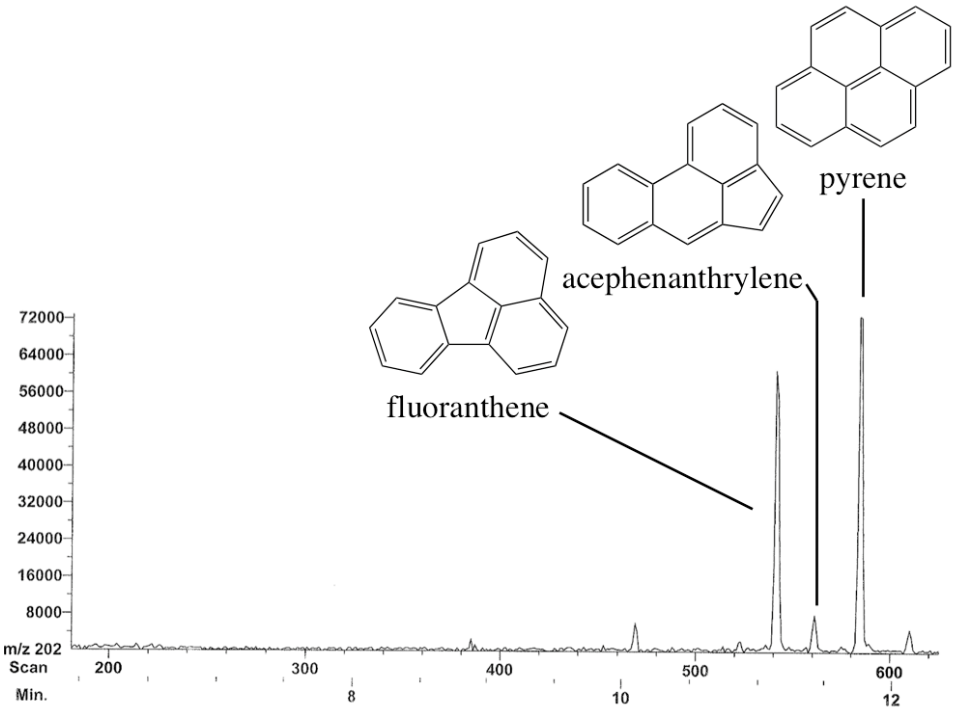

Figure S3. Extracted ion chromatogram of m/z 202 ion. Acephenanthrene was formed during CVD synthesis of MWCNTs. Pyrene and fluoranthene are commonly observed in petrogenic (fluoranthene/pyrene << 1) and pyrogenic (fluoranthene/pyrene ≥ 1) emissions, but acephenanthrylene is rare (Yunker *et al*., Lima *et al*.). Acephenanthrylene quickly isomerizes to fluoranthene by thermal interconversion during pyrogenesis (Richter *et al*., Scott and Roeloffs). Acephenanthrylene was tentatively identified by its retention time (relative to fluoranthene and pyrene) and mass spectrum.

Section S5: ***Solid carbon formation during VA-MWCNT synthesis: Effects of temperature and hydrogen gas content.***

Large PAHs (≥4-5 rings) are also precursors to soot (Richter and Howard), and controlling PAH formation during VA-MWCNT synthesis may allow one to limit the co-production of sooty or amorphous carbon phases, which are interfering contaminants in many CNT-based applications. In this system, carbonaceous solids were deposited on the inner walls of the pre-heater tube, but they were not visible in the reactor tube (where VA-MWCNT growth occurred). Solid carbon deposition increased from 0.2 to 4.0 mg $g_{carbon\ feedstock}^{-1}$ as the pre-heater temperature increased from 860 to 970 ^{o}C, Table S2), but then decreased at the highest pre-heater current (2.6 mg $g_{carbon\ feedstock}^{-1}$ at 1040^{o}C). In relation to pH_2 levels, carbon deposits were highest at low pH_2 (*e.g.*, 3.6 mg $g_{carbon\ feedstock}^{-1}$ at 0.5 atm pH_2, Table 3S). Solvent extraction of the solid carbon phases yielded no detectable PAHs (< 1 ng per 10 cm of tube), but deposits in the reactor have been shown to influence CNT formation during subsequent uses (Liu *et al*.). In the absence of sorptive surfaces upstream (*e.g.*, in a tube furnace), the large PAHs and solid phases could impinge on the reactive catalyst and potentially interfere with the reaction dynamics and resultant product purity (Meshot *et al*.). These competing processes could be eliminated with selective delivery of critical CNT precursors, rather than relying on thermal generation to provide a subset of necessary reactants in a complex mixture of chemicals, some of which present ecological and occupational concerns.

Table S2. Carbonaceous deposits formed in the quartz pre-heater tube.

Pre-heater temperature (^{o}C)	Mass of solid C deposited (mg C deposited (g C feedstock)$^{-1}$)[a]
860	0.22 ± 0.02
920	1.9 ± 0.2
970	4.0 ± 0.4
1040	2.6 ± 0.3

[a]Black, carbonaceous material that was not soluble in dichloromethane/methanol (90:10 mixture, at high pressure and temperature) was formed during the thermal pre-treatment of ethylene. The partial pressure of hydrogen in these experiments was 0.8 atm.

Table S3. Carbonaceous deposits formed in the quartz pre-heater as a function of hydrogen partial pressure.

Partial pressure H_2 (atm)	Mass of soot deposited (mg C deposited (g C feedstock)$^{-1}$)[a]
0.0	3.2 ± 0.3
0.5	3.6 ± 0.4
0.8	1.9 ± 0.2

[a]Black, carbonaceous material that was not soluble in dichloromethane/methanol (90:10 mixture, at high pressure and temperature) was formed during the thermal pre-treatment of ethylene. Soot deposition was minimized at the highest partial pressure of hydrogen. The pre-heater temperature of these experiments was 920^{o}C.

Section S6: ***Additional carbonaceous materials in the effluent contribute to smog formation.***

Many (>25) other carbonaceous side products were formed during the CVD synthesis (Figures S4 and S5). Briefly, PUF extracts were analyzed by comprehensive two-dimensional gas chromatography (GC×GC; LECO Pegasus IV- Agilent 6890N; column 1: RTX-1 (15 m x 0.25 mm I.D. x 0.25 um film); column 2: SGE BPE-50 (0.9 m x 0.10 mm I.D. x 0.10 um film)). Comprehensive two-dimensional gas chromatography (GC×GC) with time of flight mass spectrometry (TOF-MS) enabled the identification of the most abundant compounds, which included styrene, indene, and indane. Substituted benzenes, indenes, and naphthalenes were also formed during the CVD synthesis of VA-MWCNTs. While no concentrations exceeded occupational health guidelines, all of these compounds can contribute to smog formation, and must be quantified with photoactive VOC fraction of the effluent.

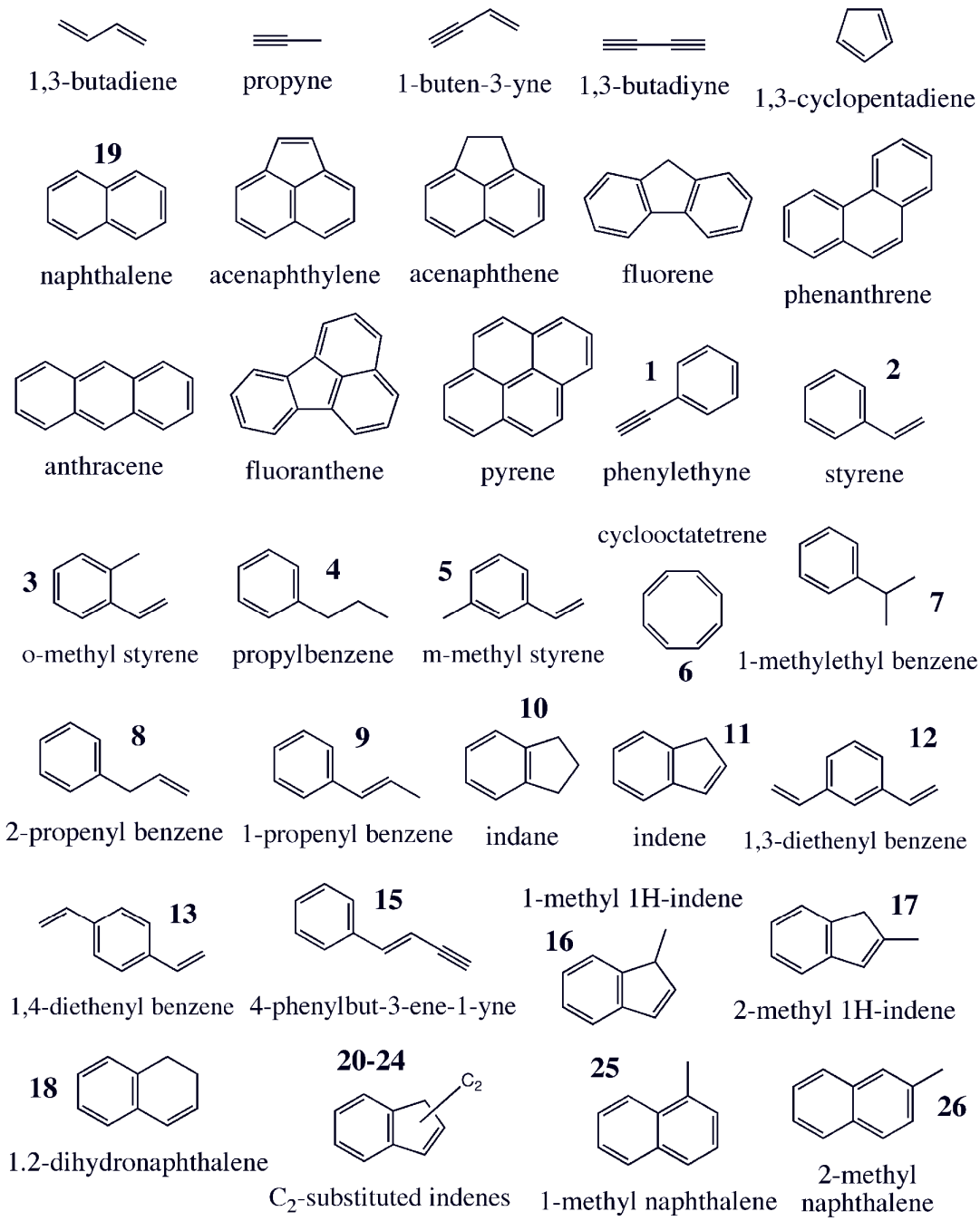

Figure S4. VOC and PAH structures of compounds identified in CVD effluent during VA-MWCNT synthesis. Bold-faced numbers refer to peak numbers that appear in Figure 9. Compounds 20 and 21 are C_2-indene isomers with no double bond in the alkyl substituent(s), whereas compounds 22-24 are C_2-indene isomers with one double bond in the alkyl chain(s). There was insufficient mass spectral information to identify compound 14, and no structure is shown.

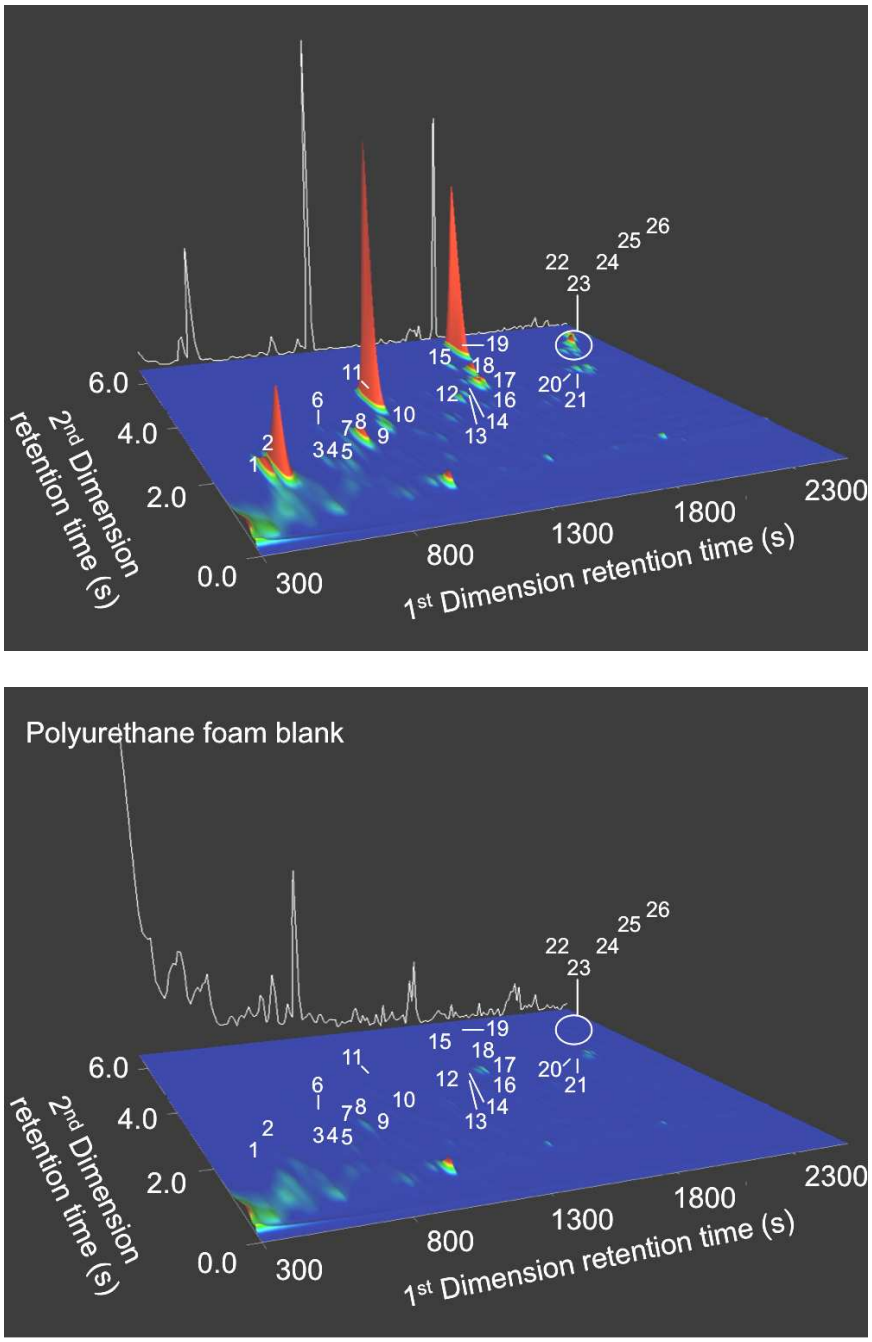

Figure S5. Comprehensive two-dimensional gas chromatogram of hydrophobic materials collected from the CVD effluent. Numbers correspond to compound identities noted in Figure S4. Here, the FID trace is shown as a three-dimensional plot and peak volume corresponds to compound abundance. A mathematically reconstructed one-dimensional trace is shown in white in the background. Compounds that were more abundant (by a factor of 3 or more) than in a blank PUF are labeled with a number. There was a series of compounds in the foreground that are unlabelled, as they are present in the PUF blank. These were alkanes (the most abundant is *n*-C_{11}) and xylenes. Note that the majority of the mass of the extract is elutes between 2 and 6 seconds in the second dimension, the "aromatic" region (Farwell *et al.*).

Section S7: *Identification of compounds formed by thermal treatment of reactant gases*

Table S4. List of compounds and analytical methods used to identify the compound.

Analytical methods (Stationary phase) Compound name	Identified and/or quantified by: GC ret. time confirmed with standard	MS spectrum consistent with standard/theory	Appropriate relative GC ret. time[a]
GC-FID (Porasil C), GC-MS-FID (DBS-624)			
hydrogen	√		
ethene (ethylene)	√	√	
1,3-butadiene		√	√ √[b]
benzene	√	√	
propene	√	√	
propyne		√	√ √
pentane	√		
1-buten-3-yne (vinyl acetylene)		√	√ √
1,2-butadiene		√	√ √
1,3-butadiyne		√	√ √
1,3-cyclopentadiene		√	√ √
butane	√	√	
propane	√		
GC-MS (HP5-MS)			
naphthalene	√	√	
acenaphthylene	√	√	
acenaphthene	√	√	
fluorene	√	√	
phenanthrene	√	√	
anthracene	√	√	
fluoranthene	√	√	
acephanthrylene		√	√
pyrene	√	√	
GCxGC-FID, GCxGC-MS (RTX-1 x SGC BPE-50)			
phenylethyne		√	√
styrene	√	√	
o-methyl styrene		√	√
propyl benzene		√	√
m-methyl styrene		√	√
cyclooctatetrene		√	√
1-methylethyl benzene		√	√
2-propyl benzene		√	√
1-propyl benzene		√	√
indane	√	√	
indene	√	√	
1,3-diethenyl benzene		√	√
1,4-diethenyl benzene		√	√
4-phenylbut-3-ene-1-yne		√	√
1-methyl 1H-indene		√	√
2-methyl 1H-indene		√	√
1,2-dihydronaphthalene		√	√
naphthalene	√	√	
C_2-substituted benzenes		√	√
1-methyl naphthalene		√	√
2-methyl naphthalene		√	√

[a]Compound's retention time is consistent with reported boiling point or relative polarity.
[b]Color of checkmark indicates instrument on which the analysis was made (*i.e.*, double checkmarks indicate that the compound was analyzed by two different instruments).

Section S8: REFERENCES

[1] Frost and Sullivan. *An Assessment on the Future of Carbon Nanotubes- Strategic Analysis of the Market and Potential.* **2007** New York, NY: Frost and Sullivan Ltd.

[2] Coll, B.F.; Dean, D.A.; Howard, E.; Johnson, S.V.; Johnson, M.R.; Jaskie, J.E. Nano-emissive display technology for large-area HDTV. *Journal of the Society for Information Display* **2006**, *14 (5)*, 477-485.

[3] Euromonitor International. Global Market Information Database: Consumer Electronics. **2007**. London, UK: Euromonitor International Plc.

[4] Gschwend, P.M.; Hites, R.A. Fluxes of polycyclic aromatic hydrocarbons to marine and lacustrine sediments in the northeastern United States. *Geochemica et Cosmochimica Acta* **1981**, *45(12)*, 2359-2367.

[5] Budzinski, H.; Jones, I.; Bellocq, J.; Piérard, C.; Garriges, P. Evaluation of sediment contamination by polycyclic aromatic hydrocarbons in the Gironde estuary. *Marine Chemistry* **1997**, *58*, 85-97.

[6] Yunker, M. B.; MacDonald, R.W.; Vingarzan, R.; Mitchell, R.H.; Goyette, D.; Sylvesre, S. PAHs in the Fraser River basin: a critical appraisal of PAH ratios as indicators of PAH source and composition. *Organic Geochemistry* **2002**, *33*, 489-515.

[7] Lima, A.L.C.; Farrington, J.W.; Reddy, C.M. Combustion-derived polycyclic aromatic hydrocarbons in the environment- A review. *Environ. Forensics* **2005**, *6*, 109-131.

[8] Richter, H.; Grieco, W.J.; Howard, J.B. Formation mechanisms of polycyclic aromatic hydrocarbons and fullerenes in premixed benzene flames. **1999**, *119*, 1-22.

[9] Scott, L.T.; Roelofs, N.H. Benzene ring contractions at high temperatures. Evidence from the thermal interconversions of aceanthrylene, acephenanthrylene, and fluoranthene. *J. Am. Chem. Soc.* **1987**, *109*, 5461-5465.

[10] Richter, H.; Howard, J.B. Formation of polycyclic aromatic hydrocarbons and their growth to soot- a review of chemical reaction pathways. *Progress in Energy and Combustion Science* **2000**, *26*, 565-608.

[11] Liu, K.; Liu, P.; Jiang, K.; Fan, S. Effect of carbon deposits on the reactor wall during the growth of multi-walled carbon nanotube arrays. *Carbon* **2007**, *45*, 2379-2387.

[12] Meshot, E.R.; Tawfick, S.; Plata, D.L.; Verploegen, E.; Hart, A.J. Decoupled thermal treatment of precursor and catalyst enables control of diameter, structural quality, and growth kinetics of vertically aligned carbon nanotubes. *ACS Nano.* **2009**, DOI:10.1021/nn900446a.

[13] Farwell, C.; Reddy, C.M.; Peacock, E.; Nelson, R.K.; Washburn, L.; Valentine, D.L. Weathering and the fallout plume of heavy oil from strong petroleum seeps near Coal Oil Point, CA. *Environ. Sci. Technol.* **2009**, *43 (10)*, 3542-3548.